

cations [1,5,7,8]. The publication of Batko and Majkut presents the purposefulness in controlling the phase images of the vibration signals as a useful tool for fault development process identification in the monitored object. The presented diagnostics method based on phase trajectories analysis determines displacement and velocity in arbitrary chosen point [2,3].

Interesting application of acoustic signal in structures defects research were presented in [4]. It shows application of the method of elastic wave propagation to detect defects in composite castings. It was proved that if a defect occurs, which is detected by the radiography, elastic wave propagation changes locally. Another example can be the photoacoustic transformation. In [15] was described the investigation of photoacoustic transformation in naturally-gyrotropic and magnetoactive crystals under internal stress by sound excitation in different modes by Bessel light beams.

This paper presents some preliminary research on possibilities of vibration signal application in research on materials. The main phenomenon useful in vibration research is resonant. Resonance vibration of materials is caused by an interaction between the inertial and elastic properties of the materials within a structure. Resonance vibration amplifies the vibration response more than the level of deflection, stress, and strain caused by static loading. Resonances are determined by the material properties, such as:

- mass,
- stiffness,
- damping properties,
- boundary conditions of the structure.

The modal research allows the frequency response function (FRF) to be determined. This describes the input-output relationship between two points on a structure as a function of frequency. Nowadays the modal testing is an effective means for identifying and simulating dynamic behavior and responses of structures. A very useful group of this research is experimental modal analysis (EMA) because this is an example of non-destructive testing. Modal research is based on vibration responses of the structures. New methods of the signal processing allows the vibrational response of the structures to the impact excitation (instrumented hammer impact excitation), which are measured, transformed into frequency response functions using Fast Fourier Transformation (FFT) [9,17]. In the practical applications the modal parameters are required to avoid resonance in structures affected by external periodic dynamic loads. Modal analysis is a process of describing a structure in terms of its natural characteristics which are the frequency, damping and mode shapes.

D. J. Mead in [14] describes some methods developed at the University of Southampton to analyze and

predict the free and forced wave motion in continuous periodic engineering structures. These kinds of methods are very commonly and used in wide research. In the paper [11] has been presented the calculation of natural frequencies vibrational analysis of composite propeller shafts and decrease of weight. The role of structural elements on the loss of total energy were investigated in [13].

The research on the nature of the wave dynamics in rod were presented in [10]. This investigation shows developed combination of finite element modeling and the transfer matrix method to solve the dynamics of the wave propagation of the periodic beam structures with defects.

Prasad and Seshu [17] investigated an experimental modal analysis of beams made with different materials such as Steel, Brass, Copper and Aluminum. The beams were excited using an impact hammer excitation technique. Some of their results were presented on figures below.

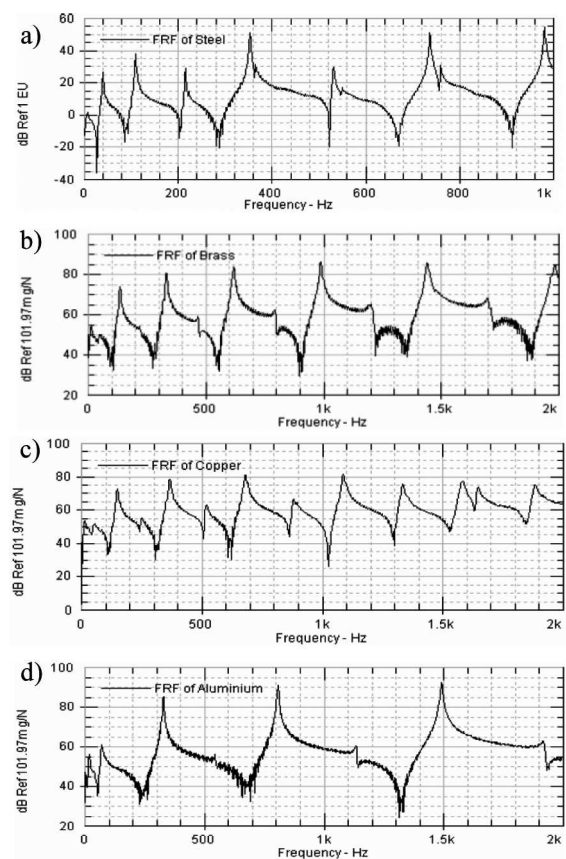


Fig. 1. Frequency response function of: a) steel, b) brass, c) copper, d) aluminum [17]

By using SDOF (Single Degree of Freedom) and MDOF (Multiple Degree of Freedom) estimation algorithms, natural frequencies and damping ratio were calculated. In SDOF and MDOF estimation the modal parameters are calculated using finite difference and quadra-

ture methods. The research shows the differences between natural frequencies, damping ratio of the materials (Fig.) and shapes of modes.

TABLE 1
EMA natural frequencies calculated by SDOF estimation algorithm using finite difference method

Mode No	Steel [Hz]	Brass [Hz]	Copper [Hz]	Aluminum [Hz]
1	40,27	40,00	24,43	70,71
2	110,34	105,52	45,21	170,29
3	216,50	224,83	150,78	329,16
4	353,72	333,61	250,108	548,42
5	532,22	469,46	367,85	808,60
6	533,75	619,46	518,46	1136,87

TABLE 2
EMA damping ratio calculated by SDOF estimation algorithm using finite difference method

Mode No	Steel [%]	Brass [%]	Copper [%]	Aluminum [%]
1	2,02	14,43	39,21	6,12
2	0,78	1,78	17,44	1,48
3	0,33	1,02	1,96	0,51
4	0,18	0,70	1,28	0,31
5	0,13	0,56	1,01	0,22
6	0,10	0,47	1,71	0,24





Mode No.	Mode.1	Mode.2	Mode.3	Mode.4
Mode shape				
Frequency	40.27Hz	110.34 Hz	216.50 Hz	353.72 Hz

Table 13. Mode shapes of steel beam in SDOF (quadrature method)





Mode No.	Mode.1	Mode.2	Mode.3	Mode.4
Mode shape				
Frequency	41.07 Hz	110.00 Hz	216.25 Hz	353.75 Hz

Fig. 2. Modal shapes of steel beam

3. Materials studied

The subject of the studies was propagation of vibrations in structural materials used in automotive vehicles. The vibrations generated while a vehicle is moving may exert a negative impact on the driving comfort and safety [7,16]. One of the most crucial systems conditioning the driving safety is the braking system. The authors undertook tests of the oscillatory wave propagation in a

braking system's structural component, i.e. a brake disk. It is responsible for a transfer of the heat and force loads which may be affected by the vibrations excited in the material structure. Such components are most frequently made of grey cast iron. In the studies in question, two samples made of different materials, characterised by different chemical compositions as well as physical and chemical properties, were used. The first of the samples was made of grey pearlitic cast iron with uniformly arranged flake graphite as shown in Fig. 3 and 4.

Owing to good casting and self-lubricating (anti-abrasion) properties as well as good workability and high vibration damping capacity, grey pearlitic cast iron is commonly used in the automotive, engineering and railway industries. It is used in automotive vehicles for fabrication of components like piston rings, cylinder sleeves or brake disks.

The second sample was made of the ST3S grade standard quality structural steel of general application shown in Fig. 5 and 6. The aforementioned materials were used to prepare the samples for their different physical and chemical properties which exerted a direct influence on the results of the studies conducted.

TABLE 3
Chemical composition of test steel ST3S according to PB-LBCH-01

Component	Average content [%]	Relative error [%]	Absolute error +/-
C	0,2	0	0
Mn	0,58	1,72	0,01
Si	0,26	0	0
P	0,008	0	0
S	0,024	4,17	0,001
Cr	0,07	14,29	0,01
Ni	0,07	0	0
Mo	0,01	0	0
W	0	-	-
V	0	-	-
Ti	0,003	33,33	0,001
Al.c	0,05	2	0,001
Al.r	0,044	9,09	0,004
Cu	0,19	5,26	0,01
As	0,005	20	0,001
Co	0,006	16,67	0,001
Nb	0	-	-
B.c	0,0004	25	0,0001
Sn	0,011	0	0

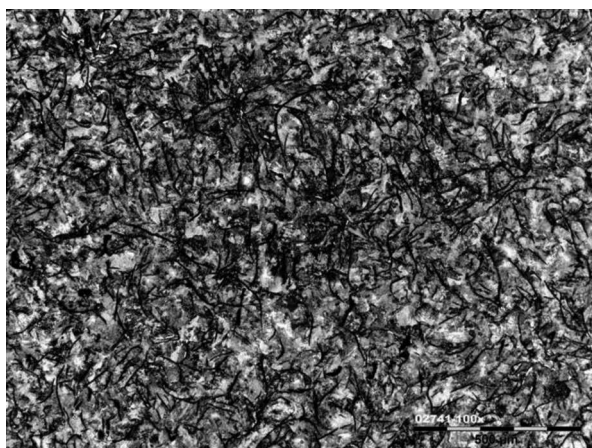


Fig. 3. Microstructure of cast iron in a sample etched in 4% nital (magnification of 100x)

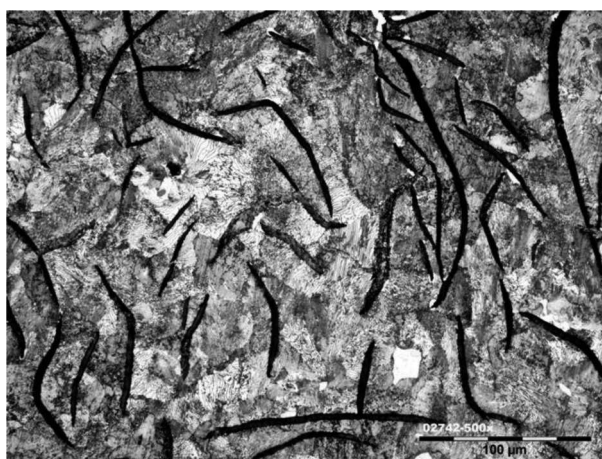


Fig. 4. Grey cast iron – pearlitic structure featuring traces of ferrite and graphite flakes, with carbon content of 2.6% and sulphur content of 0.096% (magnification of 500x)

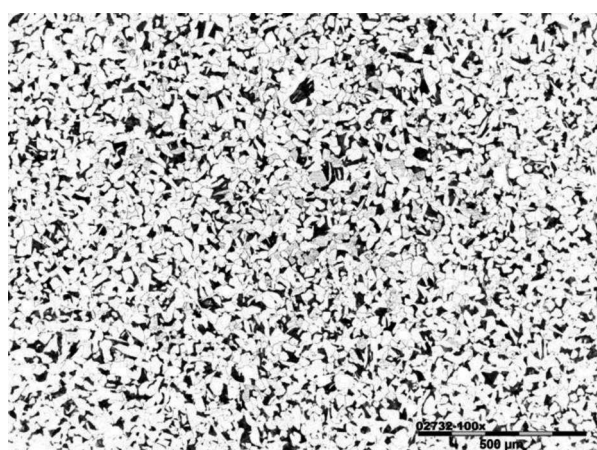


Fig. 5. Microstructure of ST3S steel in a sample etched in 4% nital (magnification of 100x)

Modern technologies applied in manufacture of metallurgical products ensure high material parameters, however, one must never exclude the possibility of a

negative impact of the inclusions from scrap processing [12] or changes in the material properties occurring in the course of manufacture or resulting from repair works such as welding [6]. The chemical composition of the ST3S steel was determined by application of emission spectrometry with spark excitation, by means of the ARL 2460 analyser and in accordance with test procedure PB-LBCH-01. The relevant test results were compared with reference standard no. 45081.



Fig. 6. ST3S steel - fine-grained ferritic-pearlitic structure (magnification of 500x)

4. Testing and analytical methods

The studies comprised structural components manufactured in accordance with the same technical documentation. The disks examined were made of various structural materials whose elemental composition was confirmed by a certified laboratory. Under the studies in question, active experiments were undertaken featuring measurements of vibration accelerations in a direction parallel to the symmetry axis of disks in two selected points the positions of which have been depicted in Fig. 7.

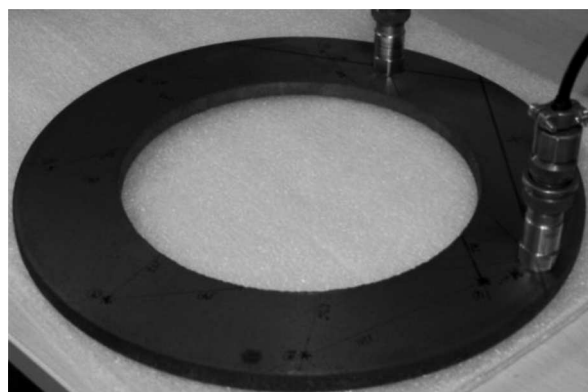


Fig. 7. Subject of studies and arrangement of measurement points

Vibration signals $x(t)$, being an effect of a single force excitation, obtained by dropping a steel ball from the height of 55 mm, were recorded. The vibrations in the disk material structure were excited by impacts in specific points whose arrangement has been depicted in Fig. 8.

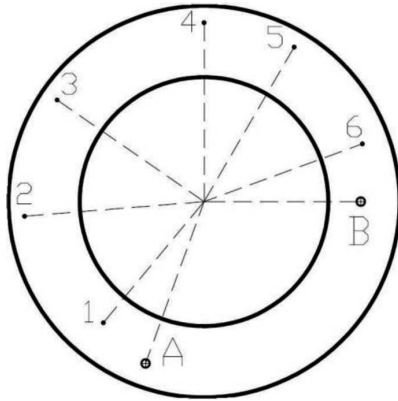


Fig. 8. Arrangement of the impulse excitation application points

In the studies discussed, a standard measurement track comprising a transducer, an A/C card and a PC was used, and the results obtained were subsequently processed in the MatLab computational environment. Consequently, specific sets of the time courses recorded for the vibration accelerations were established. A sample measurement result obtained for the impulse excitation applied has been depicted in Fig. 9.

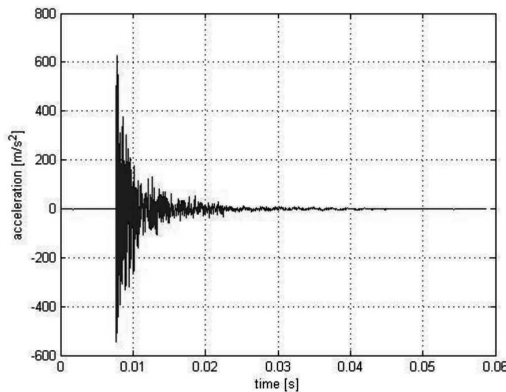


Fig. 9. Time course of vibration accelerations recorded for a cast iron disk – measurement point no. 1

The purpose of the studies undertaken was to determine the impact of the elemental composition of the material examined on the vibration energy propagation assuming geometrical conformity of the components tested. The time courses recorded provided information on the phenomenon in question, however, in order to extract it, application of the appropriate mathematical method proved necessary. The results obtained belong to a group of non-stationary signals the analysis of which forces

one to apply time-frequency methods. Simultaneous extraction of information concerning the time-frequency structure of a signal being analysed is possible owing to a wavelet transform. It is so because the wavelet function applied in this transformation can be extended or shortened. Narrow wavelets make it possible to analyse high-frequency components of a signal, and appropriately long base functions reveal its slowly-variable properties.

A wavelet transformation of signal $x(t)$ may be defined as follows:

$$WT_x(a, b) = \frac{1}{\sqrt{a}} \int_{-\infty}^{\infty} x(t) \Psi\left(\frac{t-b}{a}\right) dt$$

where:

$\Psi(t)$ – wavelet family,

a – scaling parameter effecting frequency change

$a \in R^+/0 \wedge a \sim \frac{1}{f}$, f – frequency,

$\frac{1}{\sqrt{a}}$ – wavelet normalising constant,

b – shift parameter locating the wavelet position against time axis $b \in R$.

The wavelet transform represents the correlation between the signal analysed and function $\Psi(t)$ having been appropriately scaled. The very idea of wavelet transformation is the decomposition of signal $x(t)$ into wavelet coefficients $WT_x(a, b)$ by application of the base function. As a result of such a transformation, one obtains coefficients being functions of scale and time. By altering the parameters of scale a and time shift b , one may obtain the time-frequency distribution. The base function of the wavelet transformation is subject to the operations of scaling and shifting which makes it possible to obtain wavelets of various lengths of decay time and centre frequencies. The best results are obtained by this method when wavelets adjusted in shape to the relevant signal features are used. The vibration signal processing results obtained by application of the wavelet transformation for two measurement points and different materials of the disks examined have been depicted in Fig. 10-13.

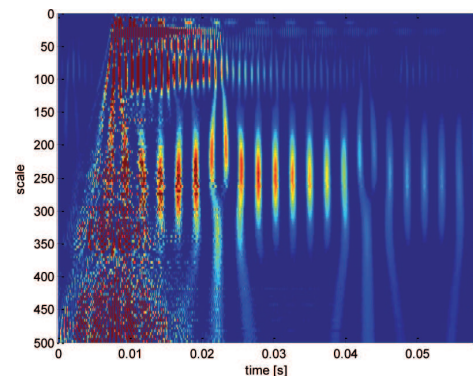


Fig. 10. Distributions of wavelet coefficients obtained for measurement point A on excitation in point 6 (steel disk)

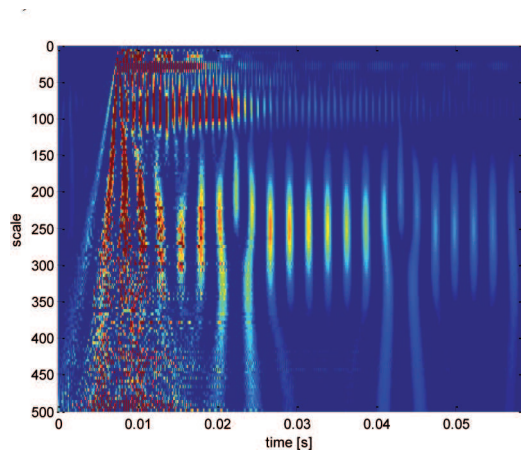


Fig. 11. Distributions of wavelet coefficients obtained for measurement point B on excitation in point 6 (steel disk)

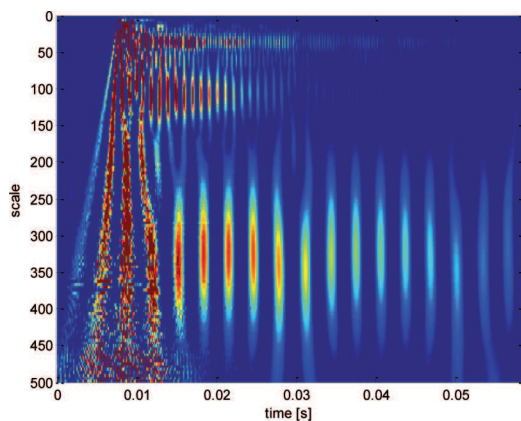


Fig. 12. Distributions of wavelet coefficients obtained for measurement point A on excitation in point 6 (cast iron disk)

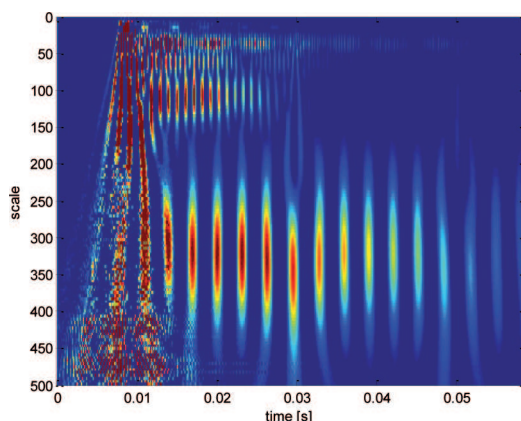


Fig. 13. Distributions of wavelet coefficients obtained for measurement point B on excitation in point 6 (cast iron disk)

The results obtained enable identification of the signal frequency constituents related to the geometry of the component being examined and the structural material type. In accordance with Heisenberg's principle of indeterminacy, distribution of wavelet coefficients in a time-scale (frequency) system constitutes a compromise

between the resolutions in both domains of the analysis. By appropriately choosing the sampling frequencies, one can match the wavelet transformation result with the chosen frequency band. Having taken the centre frequency of the wavelet applied into consideration, one may determine the free vibration frequency of the disks examined. An example of the analysis entailing the relation between the scale values and the frequency has been depicted in Fig. 14.

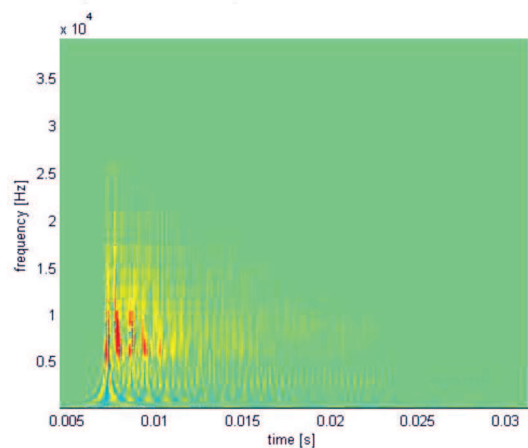


Fig. 14. Time-frequency distribution obtained for a cast iron disk – measurement point A

A result of the wavelet transformation is a matrix of wavelet coefficients enabling qualitative interpretation of properties of the materials examined. The qualitative impact assessment for the structural material the disk was made of was performed by establishing the correlograms of time sections of the wavelet coefficient matrices. The time sections applied in the analysis were chosen bearing in mind the free vibration frequencies of the components examined. Sample time sections have been provided in Fig. 15 and 16.

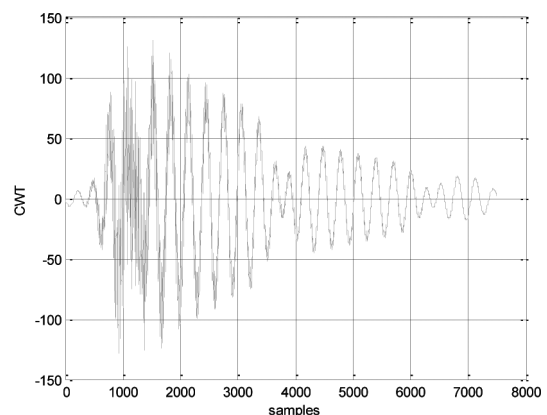


Fig. 15. Wavelet distribution time section for acceleration of the vibrations recorded by sensor A on the steel ball impact in point 1

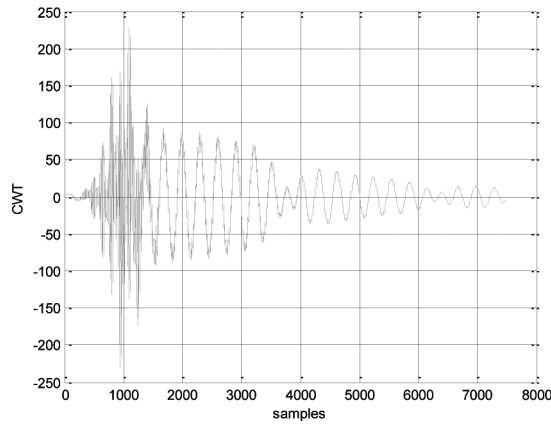


Fig. 16. Wavelet distribution time section for acceleration of the vibrations recorded by sensor B on the steel ball impact in point 1

A random signal autocorrelation function characterises the general dependency between the signal value at a certain instant and the signal value at another instant. For any chosen execution $x(t)$ of the process in question, the autocorrelation function value estimator, linking values $x(t)$ at instants t and $t + \tau$ (where τ is the shift), can be obtained by calculating the product of these values and subsequently averaging it within the observation time range of T . When T is approaching infinity, a precise value of the autocorrelation function is calculated. This function is always real and even, and its maximum is at the point corresponding to a zero shift and may assume both positive and negative values. An cross-correlation function established for various random signals is a measure of their mutual dependency. It is defined as follows:

$$R_{xy}(\tau) = \lim_{T \rightarrow \infty} \frac{1}{T} \int_0^T x(t)y(t + \tau) dt$$

This function constitutes an efficient tool for detection of predetermined processes (in the case of a random process, on high shift values, the autocorrelation function is approaching zero, whereas for a harmonic signal or other predetermined signals, the autocorrelation function does not fade as the shift value increases). When the aforementioned transformation is applied in the analysis of wavelet sections, the relevant function is as follows:

$$R_{A,B}(t_u) = \lim_{T \rightarrow \infty} \frac{1}{T} \int_0^T WT_A(t)WT_B(t + t_u) dt$$

where: A, B – indices of the measuring sensors mounting points, $WT_x(t)$ – time sections of matrices of wavelet coefficients, t_u – time shift

A sample correlogram obtained for a steel disk excited to vibrate at the first impulse excitation point has been depicted in Fig. 17.

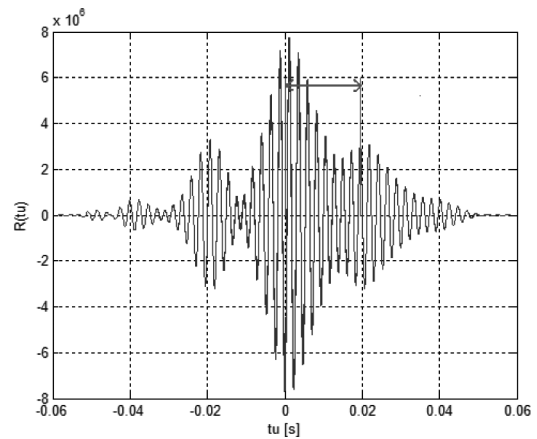


Fig. 17. Correlogram of wavelet sections with the time shift value marked on which the local maximum of the intercorrelation function occurs

The assessment of the impact exerted by the elemental composition of the material studied on the vibration energy propagation in the components examined was performed based on an analysis of the time shift values for which local maxima of the intercorrelation function occur as determined for the chosen free vibration frequencies. Both time shifts and their graphical representations have been provided in Table 4 and Fig. 18 respectively.

TABLE 4

Values of time shifts of the correlograms

Number of the impulse excitation application points	Values of time shifts of local maximum of the correlograms for steel for the frequency 409,5 [Hz]	Values of time shifts of local maximum of the correlograms for cast iron for the frequency 2736 [Hz]
1	0,0199 [s]	0,01 [s]
2	0,017 [s]	0,007 [s]
3	0,0164 [s]	0,0025 [s]
4	0,0151 [s]	0,0005 [s]
5	0,0182 [s]	0,0025 [s]
6	0,0195 [s]	0,0067 [s]

The symmetry observed in the diagram is due to the arrangement of the excitation points of the force affecting the component examined. The time delay values, constituting one of the arguments of the cross-correlation function, are a measure determining the type of the material studied. The local correlogram maxima occur for the given material on specific modes of free vibrations. If geometric conformity of the components examined and the test conditions is maintained, one may assume that the results obtained are indeed the measure of material properties.

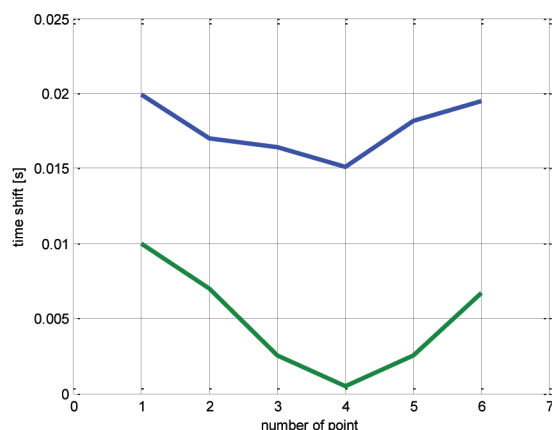


Fig. 18. Time shifts of the local maxima of the correlograms obtained for the materials examined on different free vibration frequencies. Blue – steel, green – cast iron

5. Summary

The method discussed enables analysis of the phenomena related to the impact of physical and chemical material properties on the propagation of vibration energy in a mechanical structure. The prerequisite of comparability of results is that geometric conformity of the components examined is maintained. The capabilities of the material testing method proposed should be complemented with an analysis of the influence exerted by percentage changes in the fractions of constituent elements of the given material as well as the type of the thermal and chemical processing method applied.

REFERENCES

- [1] J. Adamczyk, W. Cioch, P. Krzyworzeka, Diagnosing of rotating machinery operating under variable conditions, *The Naval Academy Scientific Papers* **48**, 169 K/1, The Naval Academy Academic Press, 9-15 (2007).
- [2] W. Batko, L. Majkut, Classification of Phase Trajectory Portraits in the Process of Recognition the Changes in Technical Condition of Monitored Machines and Constructions, *Archives of Metallurgy and Materials* **55**(3), 757-762 (2010).
- [3] W. Batko, L. Majkut, The phase trajectories as the new diagnostic discriminants of foundry machines and devices usability, *Archives of Metallurgy and Materials* **52**(3), 389-394 (2007).
- [4] Bejger, K. Gawdzinska, Identification of structural defects of metal composite castings with the use of elastic waves, *Archives of Metallurgy and Materials* **56**(1), 129-133 (2011).
- [5] R. Burdzik, Ł. Konieczny, Diagnosing of shock-absorbers of car vehicles at changeable pressure in tires, *Diagnostyka* **3**(51), Polish Society of Technical Diagnostics, 27-32 (2009).
- [6] R. Burdzik, T. Węgrzyn, Effect of Mn and Mo on the quality of welding trucks steel supporting structures, *Journal of Achievements in Materials and Manufacturing Engineering JAMME* **43**(1), 276-279 (2010).
- [7] R. Burdzik, The research of vibration of vehicle floor panel, *Silesian University of Technology Scientific Papers, s. Transport* **67**, Silesian University of Technology Academic Press, 23-30 (2010).
- [8] R. Dolecek, J. Novak, O. Cerny, Experimental research of harmonic spectrum of currents at traction drive with PMSM, *Radioengineering* **20**(2), Czech Republic (2011).
- [9] W.G. Halverson, D.L. Brown, Impulse technique for structural frequency response testing, University of Cincinnati, Reprinted from *Sound and Vibration*, (1977).
- [10] Jia-Yi Yeh, Jiun-Yeu Chen, Chen-Yang Liu, Chih-Chieh Chang, Control of Wave Propagation in Periodic Structures Having Defects, *Journal of Science and Engineering Technology* **3**(3), 45-50 (2007).
- [11] M.R. Khoshhravan, A. Paykani, A. Akbarzadeh, Design and modal analysis of composite drive shaft for automotive application, *International Journal of Engineering Science and Technology* **3**(4), 2543-2549 (2011).
- [12] J. Łabaj, B. Oleksiak, G. Siwiec, Analysis of the options of copper removal from liquid iron by evaporation, *Metalurgija* **50**(3), 173-175 (2011).
- [13] Magala, M. Schoeller, J. Tautzb, J. Casasc, The role of leaf structure in vibration propagation, *Journal of the Acoustical Society of America* **108**(5), 2412-2418 (2000).
- [14] D.J. Mead, Wave propagation in continuous periodic structures: research contributions from Southampton 1964-1995, *Journal of Sound and Vibration* **190**(3), 495-524 (1996).
- [15] G.S. Mityurich, M. Aleksiejuk, P. Rana-chowski, I.M. Pelivanov, A.N. Serdyukov, Photoacoustic diagnostics of inhomogeneous gyrotropic materials with internal stress using bessel light beams, *Archives of Metallurgy and Materials* **56**(4), 1235-1242 (2011).
- [16] J. Piecha, T. Węgrzyn, Transactions on Transport Systems, Telematics and Safety, [in:] Burdzik R.: Research of the vibration in 3 axes of car body for different idle gear rotational speed, Silesian University of Technology Academic Press, 203-214 (2011).
- [17] Ravi Prasad, D.R. Seshu, A study on dynamic characteristics of structural materials using modal analysis, *Asian Journal of Civil Engineering* **9**(2), 141-152 (2008).